JOURNAL OF MATERIALS SCIENCE 21 (1986) 3413–3419

Aluminium alloy–silica sand composites: preparation and properties

A. K. GUPTA, T. K. DAN, P. K. ROHATGI
Regional Research Laboratory (CSIR), Hoshangabad Road, Habibganj Naka, Bhopal 462026, India

Ceramic particulate composites containing up to 25 wt% silica sand in commercially pure aluminium (LM-0) and its eutectic silicon alloy (LM-6) were prepared by liquid metallurgy techniques. Pre-treated sand particles of sizes ranging from −180 to +90 μm were added to the alloy melts, followed by pouring the resulting mix into permanent moulds. Quantitative metallographic examination revealed that sand particles were uniformly distributed in both types of cast composite. Scanning electron microscopic examination of the composites showed voids around the sand particles. Tensile specimens, when fractured in an Instron machine, showed an interfacial mode of failure of the composite without affecting the sand particles, indicating poor bonding with the matrices. The hardness of LM-0 alloyed with magnesium increased from 52 to 78 BHN, whereas the ultimate tensile stress (UTS) decreased from 92 to 62 MPa as a result of the addition of 20 wt% sand particles. In the case of LM-6–sand composites, the hardness remained almost constant but the UTS decreased from 184 to 112 MPa with the addition of 20 wt% sand particles. The compressive strength of both types of composite also decreased as a result of sand additions. However, a favourable effect of magnesium alloying on the strength of the cast composite was also observed.

1. Introduction

With present-day trends of using lightweight and inexpensive materials for a variety of engineering applications, aluminium alloy ceramic particulate composites may find special applictions as they exhibit a wide range of physical and mechanical properties. Soft particles such as graphite, talc, mica and rice husk ash have been successfully dispersed in aluminium alloys by liquid metallurgy techniques for antifriction applications [1–5]. Similarly, aluminium alloy composites containing hard ceramic particles like silicon carbide, alumina, zircon sand and silica sand [6–11] have been synthesized for anti-abrasion application. The mechanical [12] and wear [13, 14] properties of some of the composites have been extensively studied.

Silica sand, the most abundantly available material on the Earth's crust, was found to be a promising ceramic material owing to its high hardness, high compressive strength, thermal stability and light weight; moreover it is cheap and easily available.

Attempts have been made, therefore, to introduce a small amount (1 to 2.5 wt%) of silica sand particles [11] into aluminium-based alloys. The particles were introduced in the vortex created by mechanical stirring of the melts above their liquidus temperature.

Of late, similar attempts have been made as a part of our major task for developing hard, ceramic particulate, aluminium alloy-based composites containing higher weight fractions of silica sand particles in various aluminium alloy-based matrices, depending upon their applications. The present work deals with the dispersion of silica sand collected from the Narmada river basin of Madhya Predesh, India in aluminium-based alloys (LM-0, LM-6).

The process parameters, namely melt temperature, impeller speed, particle size and its treatment for the preparation of 25 kg of cast composite have been assessed. Mechanical and physical properties of these composites such as tensile strength, compressive strength, hardness, and quantitative distribution of the particles in the matrix have been studied. The mode of failure and interfacial bonding of the particles with the matrix have also been observed under a scanning electron microscope.

2. Experimental procedure

2.1. Materials used

Silica sand samples from the Narmada river basin in Madhya Pradesh (India) were used. The sieve analysis and some of the physical properties are given in Tables I and II, respectively. The density of the sand

TABLE I Sieve analysis of as-received river sand

Sieve size (μm)	Content (wt %)
+425	0.20
−425 +300	1.13
−300 +212	44.66
−212 +180	7.41
−180 +150	16.90
−150 +125	11.12
−125 +90	16.92
−90 +63	0.60
−63 +45	0.0
−45	1.06

0022–2461/86 $03.00 + .12

TABLE II Properties of silica sand

Mineral	Quartz (SiO_2)
Density ($g\,cm^{-3}$)	2.6561
Crystal structure (β-quartz)	Hexagonal
Melting point (° C)	1710
Polymorphic transformation	α-quartz $\underset{\text{Vol. 1.6}}{\overset{573^\circ C}{\rightleftharpoons}}$ β-quartz $\underset{\text{Vol. 1.5}}{\overset{870^\circ C}{\rightleftharpoons}}$ β-tridymite $\underset{\text{Vol. 4.7}}{\overset{1470^\circ C}{\rightleftharpoons}}$ β-crystobolite $\xrightarrow{1740^\circ C}$ Melt
Microhardness value (VHN)	750 to 850
Mohs hardness value	7
Compressive strength (MPa)	476
Availability	Abundant, forms 12% of the Earth's crust.
Production in India, 1980 (thousand tonnes)	1180.0
Price (Rs. per kg)	0.1

was $2.6165\,g\,cm^{-3}$ and the average particle size was in the range -180 to $+90\,\mu m$.

The basic constitutent of the sand is quartz mineral or silica of chemical composition SiO_2. Apart from quartz mineral it also contains feldspar, mica, alkaline oxides and argillaceous minerals. The chemical analysis of the sand is given in Table III.

The chemical analysis of the base aluminium alloys is given in Table IV.

2.2. Pretreatment of the sand particles

In order to remove all the argillaceous materails the batch of as-received sand was leached with 0.5 wt % NaOH solution at least five times and then finally washed with fresh water to remove all the traces of NaOH solution. The washed sand was then dried at $180 \pm 20^\circ C$ in an electric oven. The dried, washed sand so obtained was then sieved for -180 to $+90\,\mu m$ size particles.

2.3. Preparation of the composites

A pre-weighed (25 kg) quantity of either commercially pure aluminium (LM-0) or LM-6 alloy was melted in a graphite crucible in a coal-fired circular pit furnace. The melt was then degassed by dry nitrogen and the oxide scum thus formed was skimmed off from the molten surface. The temperature of the molten metal was measured using a chromel–alumel thermocouple. After attaining the required temperature, molten metal was stirred mechanically and a pre-weighed amount of the treated sand particles was added slowly to the tip of the vortex. Stirring was continued till the addition of sand was completed. The molten suspension was cast into metallic moulds. For pure aluminium (LM-0), 2.5 wt % Mg was added to observe its effect on the strength of the cast composites.

2.4. Macro- and microscopic examination

Quantitative assessments of the distribution of the sand particles were made by measuring the inter-particle spacing on polished and etched specimens of the composites containing different weight fractions of sand particles at $100\times$ magnification.

Further microscopic examinations were also conducted on polished and etched specimens of the composites using optical and scanning electron microscopes so as to understand the nature of the distribution of sand particles.

TABLE III Chemical analysis of as-received river sand

Constituents	Content (wt %)
SiO_2	93
Al_2O_3	4.50
Fe_2O_3	0.40
Clay	1.0
MgO, CaO, K_2O and TiO_2	Remainder
Loss on ignition	1.0

2.5. Recovery

To assess the amount of retained sand particles in the composites, quantitative gravimetric chemical analyses were carried out by dissolving the aluminium metal matrix in an acidic solution containing equal parts of HCl, C_2H_5OH and water [15].

2.6. Mechanical and physical properties

Properties of the composites such as ultimate tensile stress (UTS), compressive strength and hardness were measured using an Instron Model 1185 and a Brinell hardness testing machine, respectively. Fractured surfaces were examined in a JEOL 35CF scanning electron microscope.

3. Results and discussion

3.1. Qualitative analysis of the behaviour of silica sand particles in the molten alloys

The foremost criterion for retaining ceramic particles in a molten metal depends upon the wettability characteristic of the particles. In the present study, uncoated silica particles were introduced into aluminium-based alloy, and the interfacial tension was reduced [17] through reaction between uncoated solid silica particles and the molten aluminium alloy

TABLE IV Chemical composition of base alloys

LM-0	Elements	LM-6
99.60	Al	Rest
0.13	Si	10–13
0.33	Fe	0.6
0.09	Cu	0.1
0.02	Ti + V	–
0.01	Mn + Zr + Cu	–
–	Mg	0.1
–	Mn	0.5
–	Ni	0.1
–	Zn	0.1
–	Zn	0.11
–	Pb	0.10
–	Sn	0.05
–	Ti	0.2

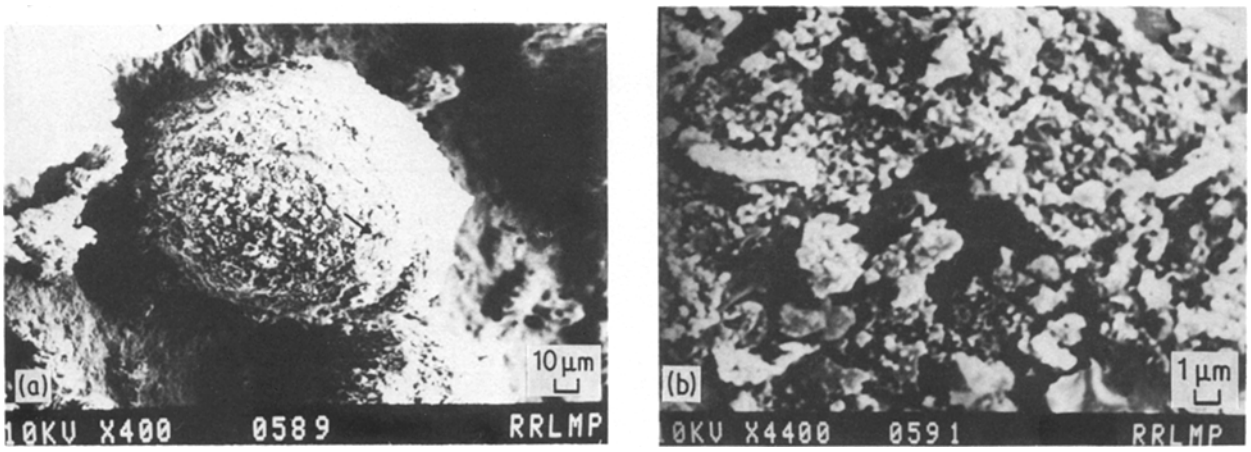

Figure 1 SEM micrographs showing (a) crystalline silicon on the extracted sand particles, (b) magnified view of the region marked by an arrow in (a).

[18]:

$$Al + SiO_2 \rightarrow Al_2O_3 + Si \quad \text{(exothermic reaction)}$$

Molten aluminium reacts with silica particles at 723 K and forms crystalline silicon at the interface. The extracted sand observed under scanning electron microscopy indicated the presence of crystalline silicon on the surface of the sand particles (Figs 1a and b) Moreover, from Fig. 2 it can be seen that most of the as-received sand particles were angular shaped, but they became sub-angular and round in shape (Fig. 3a) as a result of the interfacial reduction of SiO_2 by molten aluminium alloy. Thus the wettability is improved as a result of interfacial reaction between sand particles and molten metal.

3.2. Qualitative and quantitative examination of the dispersion of sand particles in the cast composite alloys

Typical photographs of the composite casting (Figs 4a and b) clearly revealed a uniform distribution of the sand particles in aluminium alloy without any depleted zone along and across the section. Polished specimens af LM-0 and LM-6 composites containing 20 wt % sand deeply etched with Keller's solution were also examined under SEM, which clearly revealed the uniform distribution of the sand particles (Figs 5 and 6).

The interparticle spacing (D) of sand particles in the cast composites of 20 and 7 wt % sand in LM-6 matrix (Figs 7a and b, respectively) were measured using quantitative metallography techniques and the results are shown in Table V. The maximum frequency of interparticle spacing was observed to be close to the average mean interparticle spacing, indicating a uniform distribution of particles.

Most of the sand particles were entrapped in the last freezing zone, as shown in Fig. 8, because the sand particles were pushed ahead by the solid–liquid interface into the interdendritic region. This can be explained because the heat diffusivity $(\lambda C\varrho)^{1/2}$ (where λ is the thermal conductivity, C the specific heat and ϱ the density of the particle) is less than that of the liquid matrix; the ratio $(\lambda C\varrho)^{1/2}_{\text{particle}}/(\lambda C\varrho)^{1/2}_{\text{liquid}}$ evaluated under the present experimental conditions was found to be 0.282 and 0.181 for LM-0 and LM-6 matrices, respectively. Values of the ratio which are less than one indicate the rejection of particles by the solid–liquid interface [19].

3.3. Recovery of sand particles from the cast composites

Results for the recovery of sand particles from the composites (Table VI) indicated a lower recovery of sand from LM-6 matrix in comparison with LM-0 matrix. This is most probably because of more reduction of silica sand (SiO_2).

Figure 2 SEM micrograph of as-received river sand showing particle size, shape and surface.

Figure 3 SEM micrograph of extracted sand showing the reduction reaction at the surface of the particles.

TABLE V Statistical distribution of sand particles in cast LM-6 metal-matrix composites

Sand (wt %)	Mean interparticle spacing, D	Standard deviation	Coefficient of variation
7	320	221	0.690
20	225	168	0.746

3.4. Fracture surfaces

In order to assess the nature of failure and the bonding of the sand particles with the matrix, fractured surfaces of tensile specimens were examined under SEM. Fig. 9 shows an SEM fractograph of LM-0–2.5 Mg–20 wt % sand composite, and Figs 10a and b show fractographs of LM-6–20 wt % sand composite at different magnifications. The dimples which can be clearly seen in Fig. 9 indicate a ductile matrix, whereas the tearing of the matrix shown in Fig. 10a indicates a brittle fracture of LM-6–sand composites. Further, shearing of the silicon needles around the sand particles was clearly visible at higher magnification as shown in Fig. 10b.

From the above fractographs an interfacial mode of failure was clearly seen for both composites; the interfaces were too weak to permit a transfer of load from matrix to sand particles, thus indicating a poor bonding with the matrix. Moreover, voids were also seen around the sand particles in both composites (Fig. 10b). This was due to the following reasons:

(a) Poor wettability with the parent metal, though silica sand particles were reduced by the molten aluminium alloy.

(b) Air entrapment by the particles during their addition.

(c) Most importantly, differential thermal contraction of the sand particles and the matrix occurring during solidification of the composite alloy.

3.5. Mechanical properties

Figs 11 and 12 show the BHN hardness value, ultimate tensile strength and proof compression strength of the cast composites and base alloy of LM-0–2.5 Mg and LM-6 matrices, respectively.

TABLE VI Recovery of sand particles from sand composites

Cast composites	Average measured content of sand (wt %)	Recovery of sand (%)
LM-0–2.5 Mg–20 wt % sand	16.0	80.0
LM-0–2.5 Mg–25 wt % sand	20.0	80.0
LM-6–7 wt % sand	5.3	75.7
LM-6–10 wt% sand	7.5	75.0
LM-6–15 wt % sand	11.0	73.3
LM-6–20 wt % sand	14.0	70.0
LM-6–25 wt % sand	17.5	70.0

The hardness value of composites containing 20 and 25 wt % sand in LM-0–2.5 Mg matrix was found to be 78, nearly one and a half times that of the matrix which is 52 BHN. The Brinell hardness number of LM-6 sand particulate composites containing 7 to 20 wt % particles and the base alloy remained almost constant at 65 BHN. The reason may be that in the formed composite the metal matrix–ceramic interface was strengthened by alloying with magnesium, whereas the latter composite was not alloyed with magnesium metal.

The average tensile strengths of cast composites of LM-0 containing 20 and 25 wt % sand were found to be 62 and 56 MPa, respectively. LM-0–2.5 Mg base alloy cast under identical condition showed a tensile strength of 92 MPa. In the case of LM-6 sand composites the average value of the UTS for the alloy (LM-6) was found to be 192 MPa, whereas for cast composites of the same base alloy containing 7 to 25 wt % sand the value decreased from 153 to 76 MPa, respectively. The decrease in strength of either of the cast composites was due to voids around the sand particles formed during solidification, as clearly shown in Fig. 13. The presence of such voids in the matrix would definitely make it more prone to tensile failure. During tensile loading such voids work as stress concentrators, so that the higher the quantity of voids obtained with higher particle concentration the lower will be the observed tensile strength.

The average value of the compression proof

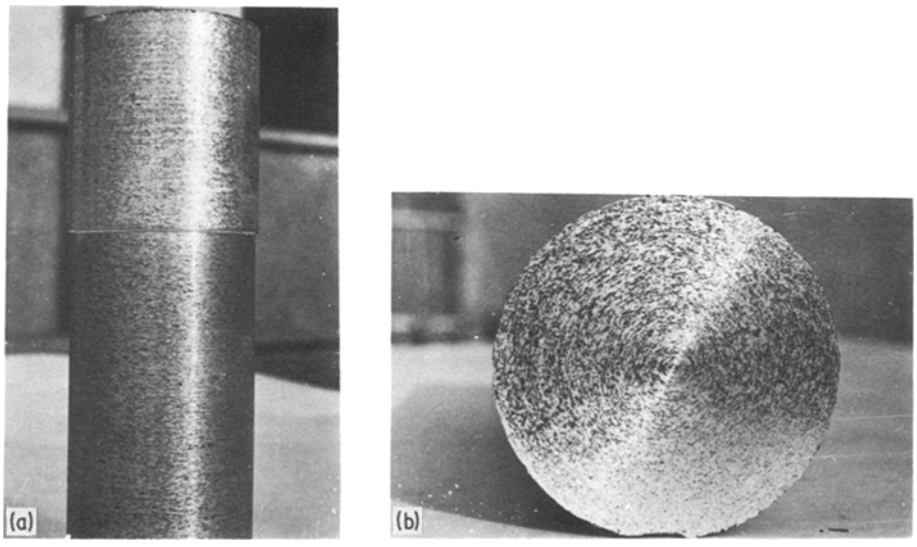

Figure 4 Photographs of a machined surface of LM-6–20 wt % sand composite casting: (a) longitudinal view, (b) cross-section.

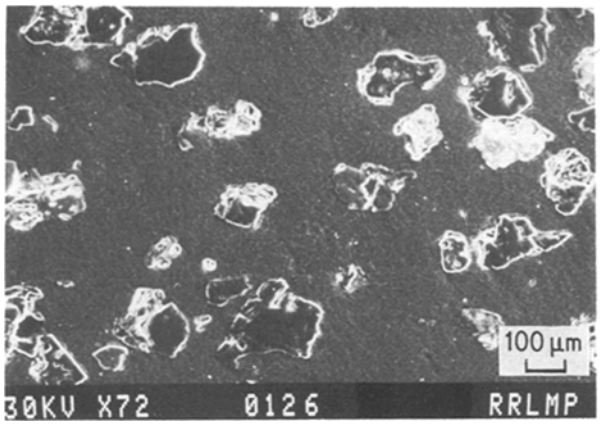

Figure 5 Scanning electron photomicrographs of LM-0–2.5 Mg–20 wt % sand showing the distribution of the sand particles.

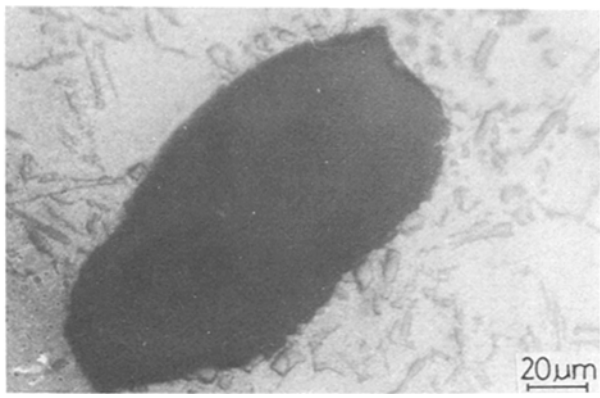

Figure 8 Optical photomicrograph of LM-6–sand composite showing the particles entrapped in the eutectic region.

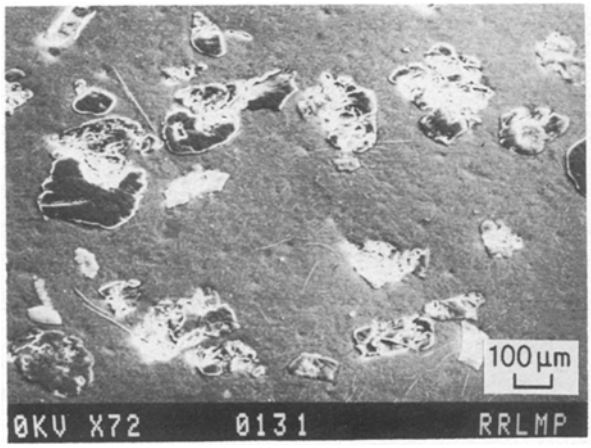

Figure 6 Scanning electron photomicrographs of LM-6–20 wt % sand composite showing the distribution of the sand particles.

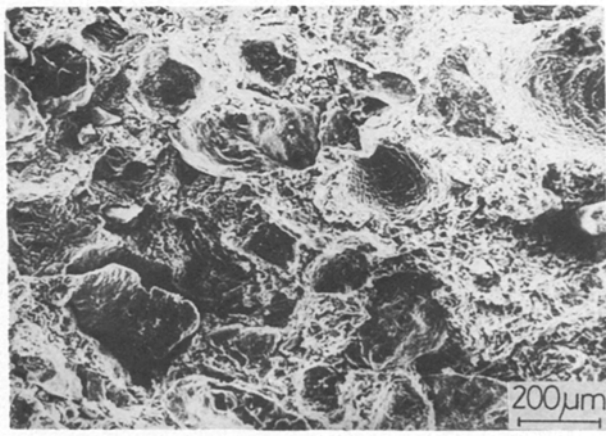

Figure 9 SEM fractograph of LM-0–2.5 Mg–20 wt % sand showing dimples indicating a ductile mode of fracture of the matrix.

strength at 0.2% strain of LM-0–2.5 Mg base alloy was found to be 200 MPa, but by the addition of 20% sand particles its value decreased to 120 MPa and it was again increased to 140 MPa in composites containing 25 wt % of sand particles. The compressive strength of the base alloy was found to be 200 MPa. A decrease in compression proof strength was observed from 150 to 120 MPa for LM-6–sand composite containing 7 to 25 wt % sand particles. The overall decreases in compression proof strength were probably due to voids present in the cast composite [20].

LM0 and LM6 alloy are presently being used for various applications such as static items of fan and pump components, latches, brake pedels, air intakes, handles etc. Composite alloys containing 15 to 20 wt % silica sand have adequate strength hardness and are more abrasion resistant, and can be substituted as potential candidates for such applications.

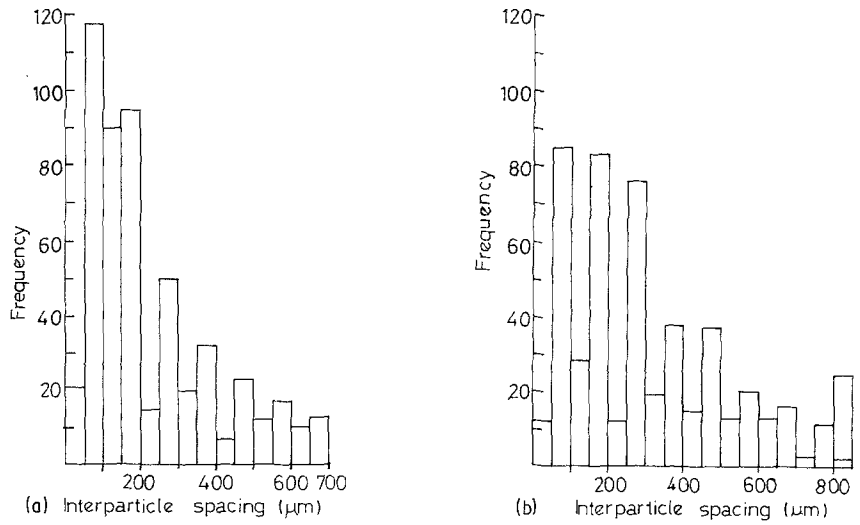

Figure 7 Histograms showing distribution of the sand particles in cast composites of LM-6 (with (a) 20 and (b) 7 wt % sand.

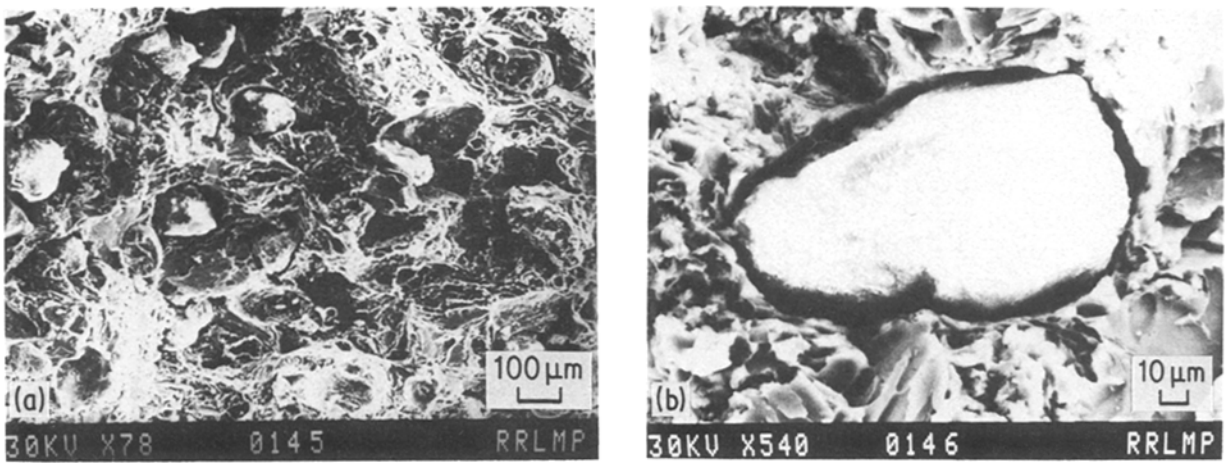

Figure 10 Scanning electron micrographs of the fracture surface of LM-6–20 wt % sand composite showing (a) brittle fracture of LM-6 matrix, (b) magnified view showing shearing of the silicon needles and void around a sand particle.

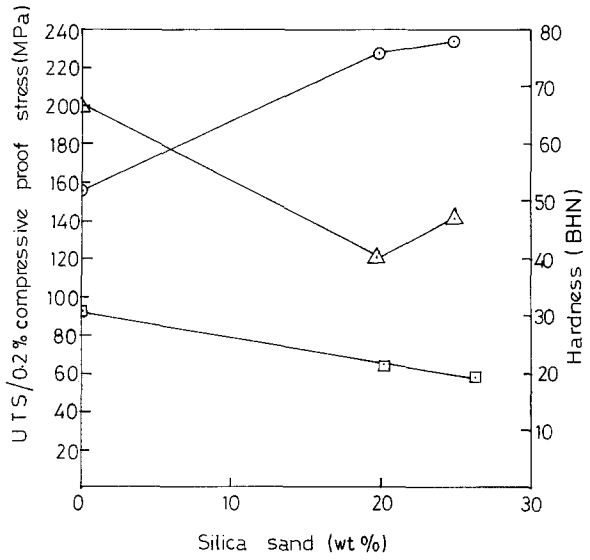

Figure 11 Mechanical properties of cast LM-0–2.5 Mg alloy and composite: (□) UTS, (△) 0.2% compressive proof stress, (○) hardness value.

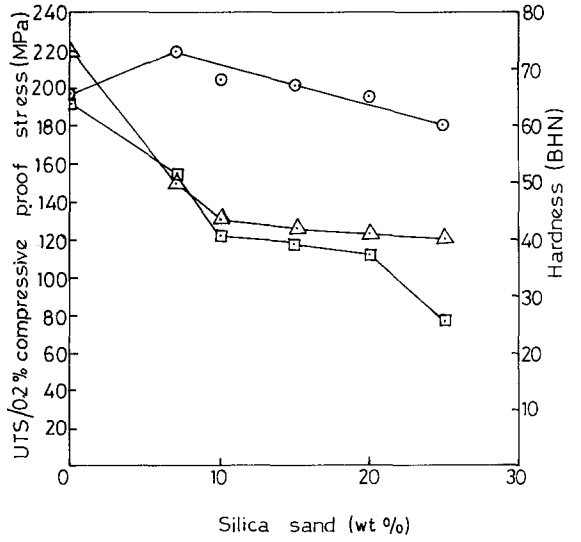

Figure 12 Mechanical properties of cast LM-6 alloy and composite (□) UTS, (△) 0.2% compressive proof stress, (○) hardness values.

4. Conclusions

1. Silica sand particles of $(-180$ to $+90)\,\mu m$ size can be uniformly dispersed up to higher weight fractions (up to 25 wt %) in aluminium alloys.

2. LM-6 sand composites have been successfully cast without alloying with magnesium, an expensive metal, which further decreases the cost of the composite. However, alloying with magnesium leads to improved strength of the cast composite.

3. Scanning electron microscopic studies showed crystalline silicon on the surface of the extracted sand particles, due to interfacial reduction by the molten aluminium metal.

4. Voids were observed under SEM which were formed during solidification of the molten suspension, and the decrease in strength such as UTS and compressive proof strength was due to such voids being present around the sand particles.

5. Silica sand can be successfully used as a filler material in aluminium alloy casting to partly replace the expensive base metal.

Acknowledgements

The authors are grateful to Drs S. V. Prasad and P. D. Ekbote for their editorial comments and Dr

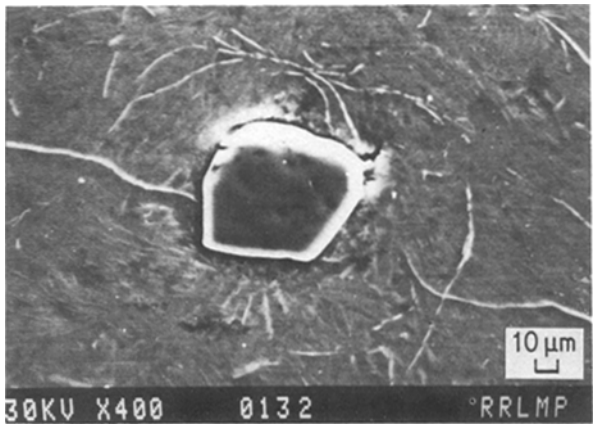

Figure 13 Scanning electron micrograph of polished and etched (Keller's reagent) surface of LM-6–sand composite showing void around a sand particle.

A. H. Yegneswaran for his valuable discussions on mechanical properties, and for performing the mechanical testing of the composites. We are indebted to Mr S. C. Arya for his assistance in the experimental work. Thanks are also due to Mr K. K. S. Gautam for his technical assistance in scanning electron microscopy.

References

1. F. A. BADIA and P. K. ROHATGI, *Trans. AFS* **76** (1969) 402.
2. *Idem, ibid.* **79** (1971) 347.
3. DEO NATH, R. T. BHAT and P. K. ROHATGI, *J. Mater. Sci* **15** (1980) 1241.
4. A. K. JHA, T. K. DAN, S. V. PRASAD and P. K. ROHATGI, *J. Mater. Sci.* in press.
5. S. DAS, T. K. DAN, S. V. PRASAD and P. K. ROHATGI, *J. Mater. Sci. Lett.* **5** (1986) 562.
6. A. SATO and R. MEHRABIAN, *Met. Trans.* **7B** (1976) 443.
7. K. J. BANSALI and R. MEHRABIAN, *J. Mater. Sci.* **34** (1982) 80.
8. F. M. HOSKING, F. FOLGAR PORTILLO and R. WUNDERLIN, *ibid.* **17** (1982) 477.
9. M. K. SURAPPA and P. K. ROHATGI, *ibid.* **16** (1981) 983.
10. A. BANERJI, M. K. SURAPPA and P. K. ROHATGI, in Proceedings of IISc National Conference on Aluminium Metallurgy, Bangalore, India, October 1979 (Indian Institute of Science, Bangalore) p. 299.
11. P. K. ROHATGI, B. C. PAI and S. C. PANDA, *J. Mater. Sci.* **14** (1979) 2277.
12. B. S. MAZUMDAR, A. H. YEGNESWARAN and P. K. ROHATGI, *Mat. Sci. Eng.* **68** (1984) 85.
13. A. BANERJI, S. V. PRASAD, M. K. SURAPPA and P. K. ROHATGI, *Wear* **82** (1982) 141.
14. M. K. SURAPPA, S. V. PRASAD and P. K. ROHATGI, *ibid.* **77** (1982) 295.
15. F. A. SCHMIDT, J. T. MASON and R. TRIVEDI, *Metallogr.* **18** (1985) 35.
16. "Smithells Metals Reference Book", edited by Eric A. Brandes, 6th Edn (Butterworths, 1983) Table 27.7.
17. A. BANERJI, P. K. ROHATGI and W. REIF, *Metallwiss. Tech.* **38** (1984) 656.
18. "The Oxide Metal Handbook" (2nd Edn), edited by G. V. Samsonov (Plenum, New York, 1983) p. 391.
19. M. K. SURAPPA and P. K. ROHATGI, *J. Mater. Sci.* **16** (1981) 562.
20. DEO NATH, PhD thesis, Indian Institute of Science, Bangalore, (1977).

Received 10 October
and accepted 21 November 1985